$E_{\kappa 3'}$, $E_{\lambda 2-4}$, and $E_{\lambda 3-1}$ and that IRF4 can enhance the transcription of genes under the control of this motif (3). For the κ-gene locus it has further been demonstrated that $E_{\kappa 3'}$ is crucial for κ–light chain secretion (14). Together, these facts could explain the defective Ig production in $IRF4^{-/-}$ mice. However, it is not likely that impaired light chain expression alone accounts for the severe B cell defect, and it is probable that IRF4 is involved in the expression of other genes that are important for late B cell differentiation.

In T cells, the deficiency of IRF4 leads to reduced proliferation and lymphokine production, and the reduced proliferation cannot be restored by exogenous IL-2. Analysis of early events after T cell activation, such as calcium influx or the expression of the activation molecules CD25 and CD69, revealed no difference between $IRF4^{-/-}$ and control T cells (7). Therefore, we conclude that IRF4 is not involved in the early events after T cell activation but is important for later processes, including both IL-2 production and IL-2 response, which is consistent with the strong up-regulation of IRF4 mRNA shortly after T cell activation (2).

Paradoxically, even though B and T cell responses are impaired in $IRF4^{-/-}$ mice, these animals develop severe lymphadenopathy. A possible explanation is that the incomplete lymphocyte activation in $IRF4^{-/-}$ mice affects the mechanisms controlling lymphocyte homeostasis, a phenomenon that has been described for IL-2– and IL-2Rα–deficient mice (15).

REFERENCES AND NOTES

1. Here we use the name IRF4, which was suggested and adopted for LSIRF by the nomenclature committee of the Genome Data Base for the gene locus in humans.
2. T. Matsuyama *et al.*, *Nucleic Acids Res.* **23**, 2127 (1995).
3. C. F. Eisenbeis, H. Singh, U. Storb, *Genes Dev.* **9**, 1377 (1995).
4. T. Yamagata *et al.*, *Mol. Cel. Biol.* **16**, 1283 (1996); A. Grossman *et al.*, *Genomics* **37**, 229 (1996).
5. M. Lamphier and T. Taniguchi, *Immunologist* **2**, 167 (1994); G. C. Sen and R. M. Ranshoff, *Adv. Virus Res.* **42**, 57 (1993); N. Tanaka *et al.*, *Nature* **382**, 816 (1996); P. S. Vaughan *et al.*, *ibid.* **377**, 362 (1995); N. Tanaka *et al.*, *Cell* **77**, 829 (1994); T. Tamura *et al.*, *Nature* **376**, 596 (1995); R. Kamijo *et al.* *Science* **263**, 1612 (1994).
6. To construct the targeting vector, an 8.4-kb Hind III fragment containing the promoter and exons 1 to 6 of the IRF4 gene was isolated from a 129J genomic library (1). The neomycin resistance cassette of pKJ1 (*neo*) [V. L. J. Tybulewicz *et al.*, *Cell* **65**, 1153 (1991)]; a Bam HI–Hind III fragment containing IRF4 exons 4, 5, and 6 (long arm); and a polymerase chain reaction (PCR) fragment of intron 1 (short arm) were sequentially cloned into pBluescript SK. The targeting vector was linearized, and E14 embryonic stem (ES) cells were transfected and selected with G418. Targeted ES cell colonies were screened by PCR with primers specific for the 3′ region of *neo* and for a genomic sequence 5′ of the targeting construct. Positive ES cell lines were verified by Southern hybridization after Hind III digestion, with the use of probes specific for a sequence 5′ of the short arm (5′ probe) or for *neo*. Out of 1500 G418-resistant colonies, we could isolate 8 with the correct mutation and with a single *neo* integration. Positive ES cells were injected into CD1 blastocysts, and chimeric offspring were mated with C57BL/6 female mice. Mice were screened by Southern blot analysis or by PCR of tail DNA with the primers 5′-GCA ATG GGA AAC TCC GAC AGT-3′ and 5′-CAG CGT CCT CCT CAC GAT TGT-3′, specific for exon 2; and primers 5′-CCG GTG CCC TGA ATG AAC TGC-3′ and 5′-CAA TAT CAC GGG TAG CCA ACG-3′, specific for *neo*.
7. H.-W. Mittrücker, unpublished observations.
8. R. Carsetti, G. Köhler, M. Lamers, *J. Exp. Med.* **181**, 2129 (1995).
9. To induce the formation of germinal centers, mice were injected intraperitoneally (ip) with sheep red blood cells (1×10^9) in 100 ml of phosphate-buffered saline (PBS) and killed 10 days later. Tissues were fixed in formalin and embedded in paraffin. Sections were stained with hematoxylin-eosin.
10. In MLR experiments, $IRF4^{+/+}$ and $IRF4^{-/-}$ spleen cells induced equal proliferation in allogeneic T cells. Furthermore, $IRF4^{-/-}$ peritoneal and spleen cells demonstrated no impairment in the processing and presentation of ovalbumin to ovalbumin-specific T cells or of LCMV peptides, after LCMV infection, to LCMV-specific T cells.
11. T. P. Leist, S. P. Cobbold, H. Waldmann, M. Aguet, R. M. Zinkernagel, *J. Immunol.* **138**, 2278 (1987); D. Moskophidis and F. Lehmann-Grube, *Proc. Natl. Acad. Sci. U.S.A.* **86**, 3291 (1989).
12. BALB/c-SCID mice (bred in-house at the Ontario Cancer Institute) were sublethally irradiated (400 rad), immediately injected intravenously with 5×10^7 spleen cells in 500 ml of PBS, and weighed every second day. In two independent experiments, 2, 5, and 10 BALB/c-SCID mice were injected with $IRF4^{+/+}$, $IRF4^{+/-}$, or $IRF4^{-/-}$ spleen cells, respectively. Mice were tail-bled, and cells were stained with mAb to H-$2K^b$ and analyzed by flow cytometry.
13. P815 cells (6×10^3 cells per mouse) were injected ip into $IRF4^{+/+}$, $IRF4^{+/-}$, and $IRF4^{-/-}$ mice (all H-2^b) and DBA/2 control mice (H-2^d). Mice (at least five mice per group) were monitored daily and killed when ascites development was visible (17 to 20 days after injection).
14. K. B. Meyer, M. J. Sharpe, M. A. Surani, M. S. Neuberger, *Nucleic Acids Res.* **18**, 5609 (1990); A. G. Betz *et al.*, *Cell* **77**, 239 (1994).
15. D. M. Willerford *et al.*, *Immunity* **3**, 521 (1995); B. Kneitz, T. Herrmann, S. Yonehara, A. Schimpl, *Eur. J. Immunol.* **25**, 2572 (1996).
16. A. Shahinian *et al.*, *Science* **261**, 609 (1993); H.-W. Mittrücker *et al.*, *J. Exp. Med.* **183**, 2481 (1996).
17. P. Mombaerts *et al.*, *Int. Immunol.* **6**, 1061 (1994).
18. T. Benatar *et al.*, *J. Exp. Med.* **183**, 329 (1996).
19. R. Schmits *et al.*, *ibid.*, p. 1415.
20. Healthy 5- to 7-week-old mice were used for all experiments. Mice were maintained according to the guidelines of the Canadian Council of Animal Care.

H.-W.M. is a recipient of a grant from the Deutsche Forschungsgemeinschaft. The authors thank M. Bachmann, G. Boehmelt, G. Duncan, D. Ferrick, C. Furlonger, D. Kägi, F. Kiefer, L. Marengere, C. Paige, J. Penninger, M. Saunders, R. Schmits, D. Siderovski, D. Speiser, S. Yoshinaga, and P. Waterhouse for providing reagents and for helpful comments.

4 October 1996; accepted 2 December 1996

Still life, a Protein in Synaptic Terminals of *Drosophila* Homologous to GDP-GTP Exchangers

Masaki Sone, Mikio Hoshino,* Emiko Suzuki, Shinya Kuroda, Kozo Kaibuchi, Hideki Nakagoshi, Kaoru Saigo, Yo-ichi Nabeshima, Chihiro Hama†

The morphology of axon terminals changes with differentiation into mature synapses. A molecule that might regulate this process was identified by a screen of *Drosophila* mutants for abnormal motor activities. The *still life* (*sif*) gene encodes a protein homologous to guanine nucleotide exchange factors, which convert Rho-like guanosine triphosphatases (GTPases) from a guanosine diphosphate–bound inactive state to a guanosine triphosphate–bound active state. The SIF proteins are found adjacent to the plasma membrane of synaptic terminals. Expression of a truncated SIF protein resulted in defects in neuronal morphology and induced membrane ruffling with altered actin localization in human KB cells. Thus, SIF proteins may regulate synaptic differentiation through the organization of the actin cytoskeleton by activating Rho-like GTPases.

The morphology of synaptic terminals changes during synaptogenesis and in response to environmental cues or neural activity (1). Rho-like GTPases, which include Rac1, Cdc42, and Rho, regulate cell motility, morphology, and adhesion through interaction with the actin cytoskeleton (2), and they are also implicated in the extension or elaboration of axons and dendrites in the nervous system (3, 4). Here we describe the Still life (SIF) proteins of *Drosophila* that participate in the signaling cascade of the Rho-like GTPases in the synaptic terminals.

To identify factors involved in the formation of neural circuits, we created *Drosophila* mutants by the insertion of an enhancer trap transposon and then screened them for reduced locomotor behavior, an approach used to identify factors that function during synapse formation (5, 6). We isolated a mutant, $sif^{98.1}$, that carries a single *P* element insertion at the cytological location 64E. Flies homozygous for this insertion demonstrated reduced locomotion (Fig. 1A) and were male sterile.

We isolated genomic DNA surrounding

the *P* element (Fig. 1B) and analyzed RNA isolated from adult heads and identified a transcript near the *P* element insertion. From several rounds of screening of adult head cDNA libraries we isolated two cDNA series, 7.9 and 9.2 kb long, corresponding to distinct start sites. A transgene prepared from the 7.9-kb cDNA, under the control of the neuron-specific *elav* promoter (*7*), rescued the behavioral phenotypes (Fig. 1A) and fertility of $sif^{98.1}$ flies. We conclude that the observed *sif* phenotypes are caused by a defect in the gene encoding the identified transcripts.

The sequences of the 7.9- and 9.2-kb cDNAs contain long open reading frames that predict proteins of 2064 and 2044 amino acids, respectively (Fig. 2, A and B) (*8*). In the NH_2-terminal portion of the 2044–amino acid protein, there is a repeated sequence and a region in which cysteines are regularly spaced (Fig. 2, B and C). These structures do not appear in the 2064–amino acid protein. The regions in common between the two sequences are homologous to the mouse TIAM-1 protein, which induces invasion of T lymphoma and is predominantly expressed in the normal brain and testis (*9*). The regions of similarity include a pleckstrin homology (PH) domain (*10*) with its COOH-terminal flanking region (55.0% identity) and a Dbl homology (DH) and another PH domain (51.2%). A potential myristoylation site, PEST sequences

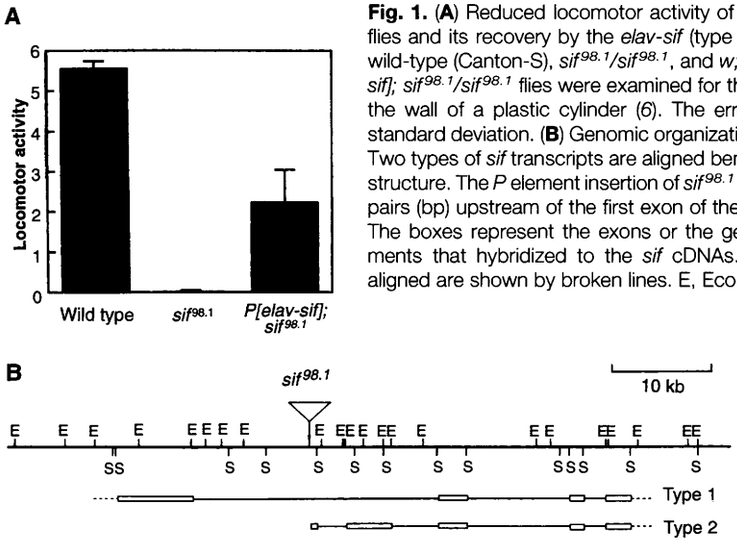

Fig. 1. (**A**) Reduced locomotor activity of the $sif^{98.1}$ mutant flies and its recovery by the *elav-sif* (type 1) transgene. The wild-type (Canton-S), $sif^{98.1}/sif^{98.1}$, and *w; P[elav-sif]/P[elav-sif]; $sif^{98.1}/sif^{98.1}$* flies were examined for their ability to climb the wall of a plastic cylinder (*6*). The error bars represent standard deviation. (**B**) Genomic organization of the *sif* locus. Two types of *sif* transcripts are aligned beneath the genomic structure. The *P* element insertion of $sif^{98.1}$ is located 44 base pairs (bp) upstream of the first exon of the type 2 transcript. The boxes represent the exons or the genomic DNA fragments that hybridized to the *sif* cDNAs. The regions not aligned are shown by broken lines. E, Eco RI; S, Sal I.

M. Sone, Department of Molecular Genetics, National Institute of Neuroscience (NIN), National Center of Neurology and Psychiatry (NCNP), 4-1-1 Ogawahigashi, Kodaira, Tokyo 187, and Department of Biophysics and Biochemistry, Graduate School of Science, The University of Tokyo, 7-3-1 Hongo, Bunkyo-ku, Tokyo 113, Japan.
M. Hoshino, H. Nakagoshi, Y.-i. Nabeshima, C. Hama, Department of Molecular Genetics, NIN, NCNP, 4-1-1 Ogawahigashi, Kodaira, Tokyo 187, Japan.
E. Suzuki, Department of Fine Morphology, Institute of Medical Science, The University of Tokyo, 4-6-1 Shirokanedai, Minato-ku, Tokyo 108, Japan.
S. Kuroda and K. Kaibuchi, Division of Signal Transduction, Nara Institute of Science and Technology, 8916-5 Takayama, Ikoma, Nara 630-01, Japan.
K. Saigo, Department of Biophysics and Biochemistry, Graduate School of Science, The University of Tokyo, 7-3-1 Hongo, Bunkyo-ku, Tokyo 113, Japan.

*Present address: Department of Neurobiology, Stanford University School of Medicine, Stanford, CA 94305–5401, USA.
†To whom correspondence should be addressed.

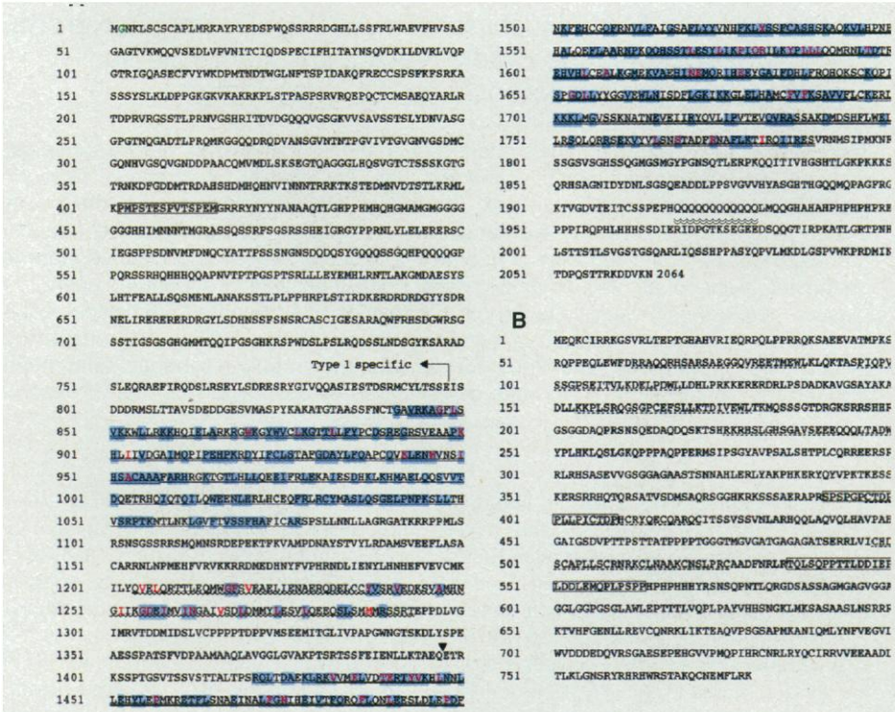

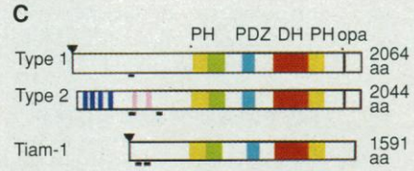

Fig. 2. The structure of the SIF proteins. (**A**) The amino acid sequence of the type 1 SIF protein (*26*). The PH domains are double-underlined, the DH domain is indicated by a bold line, and the surrounding sequences with similarity between SIF and TIAM-1 are single-underlined. The PDZ domain is marked by a wave line. In these underlined sequences, the conserved residues between SIF and TIAM-1 are indicated by blue backgrounds, and the evolutionarily well-conserved residues among several proteins (*9, 12*) are indicated by red letters. The PEST sequence is boxed (*27*). The glycine residue at position 2 shown by a green letter is a potential myristoylation site. In one cDNA clone, a nine–amino acid insertion (VTGF-CRSPQ) was observed at the position indicated by an arrowhead. The *opa* repeat is marked by a double-wave line. (**B**) The amino acid sequence of the type 2–specific region. The internally repeated sequences are marked by broken lines (amino acids 62 to 86, 94 to 118, 154 to 178, and 225 to 249). The regions in which cysteines are regularly spaced are noted by a chained line (395 to 421 and 496 to 225). The PEST sequences are boxed (*27*). (**C**) Schematic domain structures of SIF and TIAM-1. The potential myristoylation site is indicated by the arrowhead, and PEST sequences are marked with small black boxes beneath each domain structure. The dark blue bars and pink bars indicate the internally repeated structures and the cysteine-rich regions, respectively. The PH, PDZ, and DH domains and *opa* repeat are shown by yellow, light blue, red, and black, respectively. The COOH-terminal flanking region of the first PH domain has a strong homology to that of TIAM-1 and is marked by light green.

(*11*), and a PDZ domain (*12*) were also found in SIF and TIAM-1 (Fig. 2, A and C). DH domains are the conserved catalytic domains of guanine nucleotide exchange factors (GEFs) that act on the Rho-like small guanosine triphosphate (GTP)–binding proteins, converting them from the guanosine diphosphate–bound inactive state to the GTP-bound active state (*13*). TIAM-1 acts as a GEF for Rac1 and Cdc42 in vitro and for Rac1 in vivo (*14*).

We examined the expression pattern of *sif* in *Drosophila* embryos by in situ hybridization (*15*). At stage 14, several cells expressed *sif* in each segment of the central nervous system. As development proceeded, cells expressing *sif* increased in number. At stage 17, the *sif* transcripts were found only in cells in the brain and ventral nerve cord (Fig. 3A).

An antibody (AbI3) to the bacterially expressed SIF fusion protein labeled the neuropils, where neurites form synapses (*16*), in the ventral nerve cord of a stage 17 embryo (Fig. 3B) (*17*). In the body wall muscles of the third instar larva, boutons of the neuromuscular junctions (NMJs) were stained (Fig. 3C). The antibody also stained the neuropil in the adult brain (Fig. 3D). Neither the cell bodies in the cortical regions surrounding the neuropils nor the axonal processes were stained. Similar staining patterns were found in the adult brain with another antibody (AbH3) to a distinct region of SIF protein (*18*). Thus, SIF proteins were exclusively detected in the synaptic regions and predominantly at the stages when synapses had undergone maturation.

SIF proteins are localized to certain limited cytoplasmic regions of the photoreceptor axon terminals, which are mainly presynaptic (*19*), in the adult optic lobe (Fig. 3, E and F). SIF proteins are closely associated with the plasma membrane and the membrane protruding toward surrounding cells. In the larval NMJ, staining was also detected adjacent to the plasma membrane of presynaptic nerve terminals (Fig. 3G). Lateral sides of active zones of both the lamina and the NMJ were stained for SIF. Thus, SIF is localized to the submembranous region, which may affect synaptic events.

To assess SIF function, we expressed transgenes that were under the control of the *elav* promoter (*20*). We detected no abnormalities in lines carrying either of two types of intact SIF cDNAs. Because many DH domain–containing proteins express their oncogenic or invasive abilities when their NH_2-terminal portions are truncated (*9*, *13*), we constructed a truncated SIF protein (SIFΔN) lacking the NH_2-terminal sequences before the first PH domain, but containing in its place a part of the kinesin protein to ensure that the truncated protein would be localized to synapses (*21*). Lines carrying this transgene demonstrated various levels of viability, possibly correlating to the amount of expression of the transgene. In embryonic and first-larval lethal strains, the nervous system was disrupted. In the strain SIFΔN4.1, the axons of SNb, a motor neuron bundle (*22*), did not reach their target muscles in 81% of the segments examined (arrow in Fig. 4C) (*23*). In the remaining 19%, the SNb axons reached the muscles but did not develop terminal arbors, even at stage 17 when wild-type axons have normally formed arbors (arrowheads in Fig. 4, A and C). It has been reported that the constitutively active mutants of the *Drosophila* Rho-like GTPases, Drac1 and Dcdc42, display blocked axon outgrowth of peripheral neurons (*4*). These mutant proteins also interfere with the elongation of SNb axons (Fig. 4B), as observed in the truncated SIF transgenic lines. Thus, SIF protein is likely a factor in

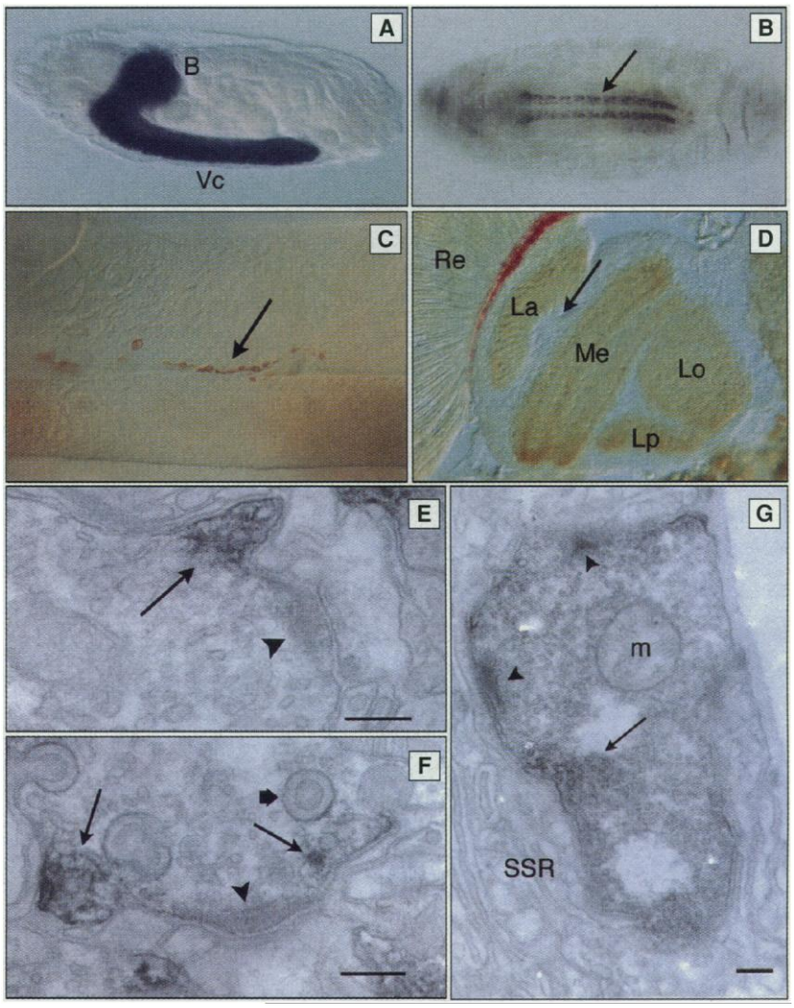

Fig. 3. Distribution of the *sif* gene products. (**A**) A lateral view of a stage 17 embryo showing the localization of *sif* transcripts. *sif* is exclusively expressed in the brain (B) and ventral nerve cord (Vc). Anterior is to the left. Panels (B) to (G) show localization of SIF proteins revealed by AbI3 staining. (**B**) Ventral view of a stage 17 embryo. Staining is observed in the neuropils (arrow), where neurites form synapses (*16*). Anterior is to the left. (**C**) The NMJ of a third instar larva. The synaptic boutons (arrow) on muscles 6 and 7 are stained. (**D**) A section of the optic lobe in the adult brain. The neuropils of the lamina (La), medulla (Me), lobula (Lo), and lobula plate (Lp) are specifically stained. The arrow indicates axon bundles of the optic chiasma. Re, retina. (**E** and **F**) Immunoelectron micrograph of the lamina. The limited regions near the plasma membrane (arrows) are stained. Note that the stained regions protrude outward. The arrowheads indicate the synaptic ribbon or density that marks the active zone. The thick arrow in (F) points to the capitate projection, a characteristic structure of the photoreceptor axon terminals (*19*). Many synaptic vesicles are visible. (**G**) is an immunoelectron micrograph of the larval NMJ. There is staining in the restricted submembranous region (arrow) next to the active zones, which are marked by synaptic ribbons (arrowheads). Many synaptic vesicles appear in the terminal; m, mitochondria; SSR, subsynaptic reticulum. Scale bars, 200 nm.

the cascade of Drac1 or Dcdc42 in the neurons.

One line with the truncated SIF, SIFΔN1.1, occasionally survived to the adult stage and was used to examine the NMJ of the third instar larva. In this line, the SNb axon bundles reached the target muscles 12 and 13 in 74% of the segments (n = 47) examined, but the patterns of their terminal arborization on the muscles were abnormal. Typically, both the terminal processes that form large (type 1) or small (type 2) synaptic boutons (*24*) were short, and the number of boutons was reduced (Fig. 4, D and E). Thus, SIFΔN disturbs the formation of synaptic arbors on target muscles.

Because Rho-like GTPases regulate cell morphology through actin fiber formation, we examined whether SIF affects the organization of the actin cytoskeleton. When expressed in human KB cells, the truncated SIF protein induced membrane ruffles (Fig. 4F) and led to the localization of actin fibers at the altered structures (Fig. 4H). This cellular phenotype resembled that induced by the constitutively active mutant of Rac1 (*25*). Furthermore, the truncated SIF protein colocalized with actin fibers (Fig. 4, F through H). Therefore, SIF protein locally affects actin cytoskeleton, possibly by activating Rac1 or its closely related GTPase in KB cells. Similar mechanisms that evoke membrane ruffling may also occur in synaptic terminals.

Our findings that the truncated SIF protein disturbs axonal extension and motor terminal arborization and induces membrane ruffling with altered actin localization imply a relevant function of intact SIF in neuronal morphology. Our data also suggest that SIF protein acts as a GEF for the Rho-like GTPases.

The subcellular localization of SIF in synapses indicates its site of function and may represent the presence of local machinery activating Rho-like GTPases that control the actin cytoskeleton. The PH and PDZ domains possibly serve SIF function in a signal cascade transduced through the plasma membrane (*10, 12*). Thus, SIF likely regulates the organization of actin-based cytoskeleton in the synaptic terminals by linking the Rho-like GTPases to the extracellular signals or to neural activity.

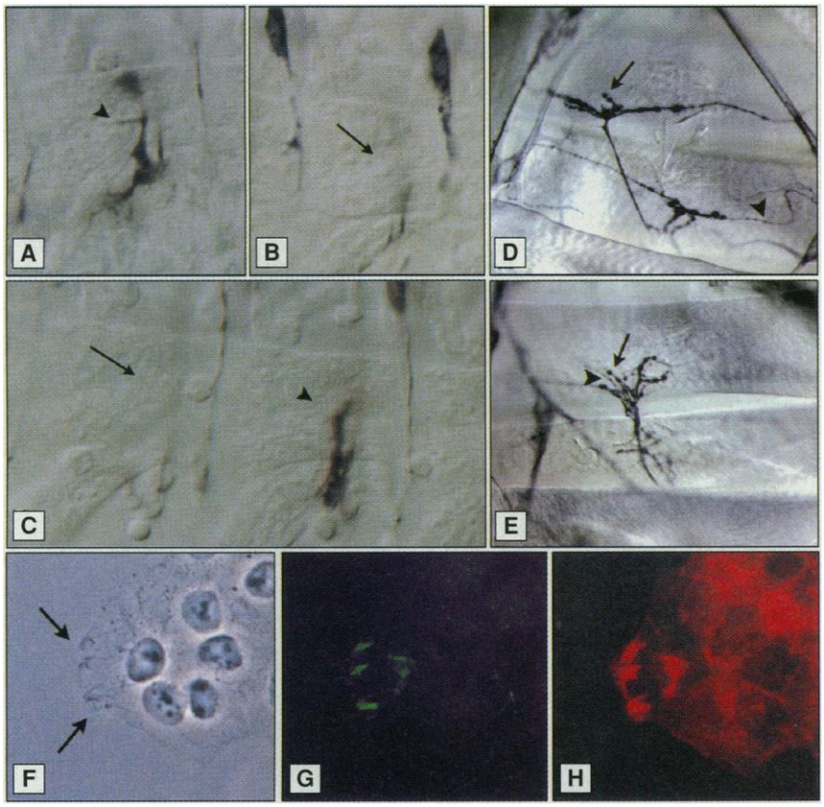

Fig. 4. The effects of the truncated SIF protein and constitutively active mutants of Rho-like GTPases on cell morphology or actin localization. In (A) to (C) the motor axons of early stage 17 embryos were detected with monoclonal antibody 1D4 (*22*). Anterior is to the left. (**A**) Wild-type (Canton-S) embryo. The SNb axon bundle is present and extends the terminal arbor between muscles 6 and 7 (arrowhead). (**B**) *elav-Gal4; UAS-Dcdc42V12.2* embryo. *Dcdc42V12* encodes a constitutively active Dcdc42 protein (*4*). The SNb axon bundle is missing (arrow). A similar phenotype was observed in the embryos that express the constitutively active Drac1 protein, Drac1V12 (*4*). (**C**) *elav-Gal4; UAS-SIFΔN4.1* embryo. In 81% of the segments (A2 to A7, n = 59) examined, the SNb axon bundle did not reach the target muscles 6 and 7 (arrow). In the remaining 19%, the SNb reached the muscles, but did not form terminal arbors (arrowhead). (**D** and **E**) Motor terminal arborization on the third instar larval muscles. Muscles 12 and 13 of the A3 segment are indicated. The motor axons and boutons are stained with antibody to horseradish peroxidase (*28*). Large type 1 and small type 2 boutons are indicated by arrows and arrowheads, respectively. Anterior is to the left. Panel (D) shows a wild-type embryo and (E) an *elav-Gal4; UAS-SIFΔN1.1* embryo. The total number of boutons on muscles 12 and 13 of the A3 segment is reduced [129 ± 34 (SD), n = 5, $P < 0.005$] when compared with the wild type (260 ± 64, n = 8). (**F** to **H**) Human KB cells expressing the truncated SIF protein (*29*). The same view was visualized with phase-contrast optics (F), fluorescein isothiocyanate (green) for the FLAG-tagged truncated SIF (G), and rhodamine (red)-phalloidin for filamentous actin (H). Note that only the cell expressing the truncated SIF shows membrane ruffles (arrows) and altered actin localization. The truncated SIF colocalizes with actin.

REFERENCES AND NOTES

1. Z. W. Hall and J. R. Sanes, *Cell/Neuron* **72/10** (suppl.), 99 (1993); M. E. Burns and G. J. Augustine, *Cell* **83**, 187 (1995); R. J. Kleiman and L. F. Reichardt, *ibid.* **85**, 461 (1996); D. C. Lo, *Neuron* **15**, 979 (1995); C. S. Goodman and C. J. Shatz, *Cell/Neuron* **72/10** (suppl.), 77 (1993).
2. A. Hall, *Annu. Rev. Cell Biol.* **10**, 31 (1994); L. M. Machesky and A. Hall, *Trends Cell Biol.* **6**, 304 (1996).
3. L. Luo *et al.*, *Nature* **379**, 837 (1996); D. J. G. Mackay, C. D. Nobes, A. Hall, *Trends Neurosci.* **18**, 496 (1995).
4. L. Luo, Y. J. Liao, L.Y. Jan, Y. N. Jan, *Genes Dev.* **8**, 1787 (1994).
5. M. Hoshino, F. Matsuzaki, Y.-i. Nabeshima, C. Hama, *Neuron* **10**, 395 (1993).
6. M. Hoshino, E. Suzuki, Y.-i. Nabeshima, C. Hama, *Development* **122**, 589 (1996).
7. The plasmid used for rescuing the $sif^{98.1}$ mutant was constructed by insertion of the type 1 *sif* cDNA into a transformation vector containing the 3.5-kb promoter fragment of the *elav* gene [K.-M. Yao and K. White, *J. Neurochem.* **63**, 41 (1994)] and the *hsp70* polyadenylate additional signal. This plasmid was introduced to *white* flies by *P* element–mediated germline transformation.
8. The nucleotide sequence data reported here will appear in the DNA Databank of Japan, European Molecular Biology Laboratory, and GenBank with the accession numbers D86546 and D86547. In both cDNAs, the nucleotide sequences around the first ATG codon match the *Drosophila* translation start consensus sequence [D. R. Cavener, *Nucleic Acids Res.* **15**, 1353 (1987)]. In the 2064–amino acid protein, an in-frame stop codon is located 54 bp upstream of the ATG codon. In the 2044–amino acid protein, the location of an in-frame stop codon 945 bp upstream of the ATG codon raises the possibility that a codon other than ATG is used as the initiation codon as previously reported for several genes [M. B. Feany and W. G. Quinn, *Science* **268**, 869 (1995)].
9. G. G. M. Habets *et al.*, *Cell* **77**, 537 (1994).
10. M. A. Lemmon, K. M. Ferguson, J. Schlessinger, *ibid.* **85**, 621 (1996).
11. M. Rechsteiner and S. W. Rogers, *Trends Biochem. Sci.* **21**, 267 (1996).
12. C. P. Ponting and C. Phillips, *ibid.* **20**, 102 (1995); J. E. Brenman *et al.*, *Cell* **84**, 757 (1996).
13. M. J. Hart *et al.*, *J. Biol. Chem.* **269**, 62 (1994); L. A.

Quilliam, R. Khosravi-Far, S. Y. Huff, C. J. Der, *BioEssays* **17**, 395 (1995).
14. F. Michiels, G. G. M. Habets, J. C. Stam, R. A. van der Kammen, J. G. Collard, *Nature* **375**, 338 (1995).
15. In situ hybridization to embryos was performed as previously described (*5*) with a single-stranded DNA probe corresponding to amino acids 870 to 1095. Embryonic stages are as previously described [J. A. Campos-Ortega and V. Hartenstein, *The Embryonic Development of* Drosophila melanogaster (Springer-Verlag, Berlin, 1985)].
16. J. T. Littleton, H. J. Bellen, M. S. Perin, *Development* **118**, 1077 (1993).
17. Two antibodies to SIF, AbI3 and AbH3, were raised to fusion proteins that consisted of portions of the SIF proteins (amino acids 327 to 604 of type 2 for AbI3 and 1080 to 1269 for AbH3) and metal-binding domains derived from pET16b (Novagen) and pTrcHis A (Invitrogen) vector, respectively. Injection of the purified proteins into rats and affinity purification of the antisera were performed as described (*6*). For immunostaining, embryos and larvae were fixed with 4% paraformaldehyde in phosphate-buffered saline for 20 min and stained with antibody to SIF using ABC Elite (Vector Labs). Preparation and staining of adult brain sections and immunoelectron microscopy were performed as described (*6*).
18. In embryos and larvae, we observed no staining with AbH3 probably because of insufficient SIF expression for the sensitivity of this antibody.
19. I. A. Meinertzhagen and S. D. O'Neil, *J. Comp. Neurol.* **305**, 232 (1991).
20. The GAL4-UAS system was used to express the transgene in the embryonic and larval nervous systems [A. H. Brand and N. Perrimon, *Development* **118**, 401 (1993)].
21. The plasmid expressing SIFΔN protein was constructed by ligating cDNA fragments encoding a portion of the kinesin heavy chain (amino acids 1 to 605) [E. Giniger, W. Wells, L. Y. Jan, Y. N. Jan, *Roux's Arch. Dev. Biol.* **202**, 112 (1993); M. F. A. VanBerkum and C. S. Goodman, *Neuron* **14**, 43 (1995)] and a portion of SIF (amino acids 838 to 2064) into the pUAST transforming vector (*20*).
22. D. Van Vactor, H. Sink, D. Fambrough, R. Tsoo, C. S. Goodman, *Cell* **73**, 1137 (1993).
23. This strain dies during the embryonic and first instar larval stages. Two other independent embryonic lethal lines carrying *SIFΔN* exhibit similar but more severe phenotypes.
24. J. Johansen, M. E. Halpern, K. M. Johansen, H. Keshishian, *J. Neurosci.* **9**, 710 (1989).
25. M. Sone *et al.*, data not shown; T. Nishiyama *et al.*, *Mol. Cell. Biol.* **14**, 2447 (1994); C. D. Nobes and A. Hall, *Cell* **81**, 53 (1995).
26. Single-letter abbreviations for the amino acid residues are as follows: A, Ala; C, Cys; D, Asp; E, Glu; F, Phe; G, Gly; H, His; I, Ile; K, Lys; L, Leu; M, Met; N, Asn; P, Pro; Q, Gln; R, Arg; S, Ser; T, Thr; V, Val; W, Trp; and Y, Tyr.
27. The PEST scores are 8.88 (type 1), 6.62 (type 2, amino acids 389 to 409), and 9.18 (type 2, amino acids 534 to 563).
28. L. Y. Jan and Y. N. Jan, *Proc. Natl. Acad. Sci. U.S.A.* **79**, 2700 (1982).
29. Microinjection of plasmid DNAs into the nuclei of KB cells was performed as previously described except that the cells were serum-starved for 30 hours [S. Kuroda *et al.*, *J. Biol. Chem.* **271**, 23363 (1996)]. The plasmid DNA, pFCMVsifΔN, used for microinjection was constructed by inserting a DNA fragment encoding portions of SIF (amino acids 1 to 18 and 838 to 2064) into pFLAG-CMV-2 (Kodak). The FLAG-SIF fusion protein was labeled with antibody to FLAG M2 (Kodak) and detected with fluorescein isothiocyanate (FITC)–conjugated antibody to mouse immunoglobulin G.
30. We thank L. Luo and Y. N. Jan for the transgenic strains carrying *Drac1* and *Dcdc42* derivatives, T. Uemura for the *elav-GAL4* strain, A. Nose for monoclonal antibody 1D4, A. DiAntonio and E. Giniger for the plasmids containing the *elav* promoter and *kinesin* gene, respectively, C.-S. Yoon for technical instruction, and S. Yoshida, A. Chiba, and all members of our department for comments and discussions. Supported by a Grant-in-Aid for Priority Area from the Ministry of Education, Science, Sports and Culture and the research grant for Nervous and Mental Disorders from the Ministry of Health and Welfare of Japan.

13 August 1996; accepted 27 November 1996

Tumor Infarction in Mice by Antibody-Directed Targeting of Tissue Factor to Tumor Vasculature

Xianming Huang,* Grietje Molema,*† Steven King, Linda Watkins, Thomas S. Edgington, Philip E. Thorpe‡

Selective occlusion of tumor vasculature was tested as a therapy for solid tumors in a mouse model. The formation of blood clots (thrombosis) within the tumor vessels was initiated by targeting the cell surface domain of human tissue factor, by means of a bispecific antibody, to an experimentally induced marker on tumor vascular endothelial cells. This truncated form of tissue factor (tTF) had limited ability to initiate thrombosis when free in the circulation, but became an effective and selective thrombogen when targeted to tumor endothelial cells. Intravenous administration of the antibody-tTF complex to mice with large neuroblastomas resulted in complete tumor regressions in 38 percent of the mice.

As a strategy for cancer therapy, the use of immunoconjugates that selectively occlude the vasculature of solid tumors offers several theoretical advantages over immunoconjugates that target tumor cells directly. First, because tumor cells depend on a blood supply, local interruption of the tumor vasculature will produce an avalanche of tumor cell death (*1*). Second, the tumor vascular endothelium is in direct contact with the blood, whereas the tumor cells themselves are outside the bloodstream and, for the most part, are poorly accessible to immunoconjugates (*2*). Third, tumor vascular endothelial cells are not transformed and are unlikely to acquire mutations that render them resistant to therapy.

We explored the feasibility of treating solid tumors by targeting human tissue factor (TF) to tumor vascular endothelium in a mouse model. TF is the major initiating receptor for the thrombogenic (blood coagulation) cascades (*3*). Assembly of cell surface TF with factor VII/VIIa generates the functional TF:VIIa complex. This complex rapidly activates the serine protease zymogens factors IX and X by limited proteolysis, leading to the formation of thrombin and, ultimately, a blood clot. A recombinant form of TF has been constructed that contains only the cell surface domain (*4*). This truncated TF (tTF) is a soluble protein with a factor X–activating activity that is about five orders of magnitude less than that of native transmembrane TF in an appropriate phospholipid membrane environment (*5*). This is because the TF:VIIa complex binds and activates factors IX and X far more efficiently when associated with a negatively charged phospholipid surface (*5*, *6*). We reasoned that, by using an antibody to target tTF to tumor vascular endothelium, the tTF would be brought into proximity with a cell surface so as to recover in part its native function and locally initiate thrombosis. Such an antibody-tTF conjugate (or "coaguligand") would selectively thrombose tumor vasculature.

To test this concept, we used a mouse model in which the tumor vascular endothelium expresses a marker that is lacking on the normal vascular endothelium (*7*). Naturally occurring markers of tumor vascular endothelium have not been identified in mice, although some strong candidates have been identified for humans (see below). In our model, C1300(Muγ) mouse neuroblastoma cells that have been stably transfected with the murine interferon-γ (IFN-γ) gene are grown as a solid subcutaneous tumor in BALB/c *nu/nu* mice. The IFN-γ secreted by the tumor cells induces local expression of major histocompatibility complex class II antigens (I-A^d and I-E^d) on the tumor vascular endothelium. Class II antigens are absent from normal vascular endothelium in mice, although they are present on B lymphocytes, monocytes, and some epithelial cells.

To target tTF to I-A^d on tumor vascular

X. Huang, G. Molema, S. King, L. Watkins, P. E. Thorpe, Department of Pharmacology and Hamon Center for Therapeutic Oncology Research, University of Texas Southwestern Medical Center, Dallas, TX 75235, USA.
T. S. Edgington, Departments of Immunology and Vascular Biology, Scripps Research Institute, La Jolla, CA 92037, USA.

*These authors contributed equally to this work.
†Present address: Groningen Utrecht Institute for Drug Exploration, Department of Clinical Immunology, and Department of Pharmacokinetics and Drug Delivery, University of Groningen, Hanzeplein 1, 9713 GZ Groningen, Netherlands.
‡To whom correspondence should be addressed.